Subsurface Eddy Facilitates Retention of Diel Vertical Migrators in a Biological Hotspot

K. Hudson[1], M.J. Oliver[1], J. Kohut[2], J.H. Cohen[1], M.S. Dinniman[3], J. Klinck[3], H. Statscewich[4], K. Bernard[5], and W. Fraser[6]

[1]College of Earth, Ocean, and Environment, University of Delaware, Lewes, Delaware, USA; [2]Department of Marine and Coastal Sciences, Rutgers, The State University of New Jersey, New Brunswick, New Jersey, USA; [3]Department of Ocean and Earth Sciences, Old Dominion University, Norfolk, VA, USA; [4]College of Fisheries and Ocean Sciences, University of Alaska, Fairbanks, Fairbanks, Alaska, USA; [5]College of Earth, Ocean, and Atmospheric Sciences, Oregon State University, Corvallis, Oregon, USA; [6]Polar Oceans Research Group, Sheridan, Montana, USA.

Corresponding author: Katherine Hudson (khudson@udel.edu)

Key Points:

- Diel vertical migration increases residence time of particles relative to near-surface particles.
- Shallow surface layers and long days lead to longer residence times.
- Increased residence times of migrators may lead to persistent food sources for higher trophic levels near biological hotspots.

Abstract

Diel vertical migration (DVM) is a common behavior in zooplankton populations world-wide. Every day, zooplankton leave the productive surface ocean and migrate to deep, dark waters to avoid visual predators and return to the surface at night to feed. This behavior may also help retain migrating zooplankton in biological hotspots. Compared to fast and variable surface currents, deep ocean currents are sluggish, and can be more consistent. The time spent in the subsurface layer are driven by day length and the depth of surface mixed layer. A subsurface, recirculating eddy has recently been described in Palmer Deep Canyon, a submarine canyon adjacent to a biological hotspot. Previous circulation model simulations have shown that residence times of particles increase with depth within this feature. We hypothesize that DVM into the subsurface eddy increases local retention of migrating zooplankton in this biological hotspot and that shallower mixed layers and longer day length would increase the time in the subsurface layer. We demonstrate that vertically migrating particles have residence times on the order of 30 days, which is significantly greater than residence times of near-surface, non-migrating particles. The interaction of DVM with this subsurface feature may be important to the establishment of the biological hotspot within Palmer Deep Canyon by retaining critical food resources in the region. Similar interactions between DVM behavior and subsurface circulation features, modulated by mixed layer depth and day length, may also increase residence times of local zooplankton populations elsewhere.

Plain Language Summary

Diel vertical migration is considered the world's largest migration. Organisms migrate into the surface to feed at night when visual predation risks are low. During the day, these organisms migrate to deeper waters to avoid predation, when visual predators like seabirds and fish are the most active and predation risks are highest. This behavior may also retain zooplankton in areas of high biological activity, or hotspots. Migration between a rapidly-moving surface layer and a sluggish subsurface layer may reduce the net movement of organisms. Since this behavior is modulated by light intensity, more daylight hours would increase the time in the slower subsurface layer and help retain zooplankton in these hotspots.

We used a biological hotspot over Palmer Deep Canyon to test how this behavior, and the factors that control the time spent in the subsurface layer, affects zooplankton retention in

hotspots. We found that retention was highest for migrators when migrations were deepest, days were long, and surface layers were shallow. Performing migrations also increased retention in hotspots relative to near-surface non-migrating particles. While we used an Antarctic hotspot as a case study, we believe that these behaviors and factors may impact retention in biological hotspots worldwide.

1 Introduction

Diel vertical migration (DVM) occurs in zooplankton and fish species across the world (Brierley, 2004). Many species of zooplankton and euphausiids perform this migration daily, migrating from great depths to the surface waters at night and migrating back down to these depths during the day (Brierley, 2004; Hays, 2008). This migration is likely a trade-off between predator avoidance and feeding (Brierley, 2004; Hays, 2008). Migrators feed at night in surface waters when visual predation is low. During the day, they migrate to depth which limits visual predation (Brierley, 2004; Hays, 2008). There are many cues that trigger DVM or control the depth of migration. These include, but are not limited to, day length (DL) (Benoit et al., 2010; Cohen & Forward, 2005; Hobbs et al., 2018, 2021), circadian rhythms (Cohen & Forward, 2005), food availability (Cresswell et al., 2009; Sha et al., 2020), ontogeny (Hays, 1995), and predation pressures (Cresswell et al., 2009; Hays, 1995; Sha et al., 2020). These cues can vary widely across species and latitudes, and within populations (Benoit et al., 2010; Conroy et al., 2020; Cresswell et al., 2009; Hays, 2008; Sha et al., 2020; Thibodeau, 2015).

While primarily believed to function in predator avoidance, DVM may increase retention of migrators in biologically productive regions, or hotspots (Batchelder et al., 2002; Carr, 2003, 2006; Emsley et al., 2005; Lavoie et al., 2000; Marta-Almeida et al., 2006; Peterson, 1998). In areas where upwelling is induced through along-shore winds and Ekman pumping, organisms are pushed offshore in surface waters. When these organisms migrate down and out of this surface layer, they could be advected back inshore by the subsurface return flow, thus retaining these organisms within the system (Batchelder et al., 2002; Peterson, 1998). This mechanism has been shown to retain crab larvae in upwelling systems off the coast of Portugal (Marta-Almeida et al., 2006) and several copepod species in upwelling systems associated with eastern boundary currents worldwide (Peterson, 1998).

Subsurface circulation features other than those associated with regional upwelling have also been shown to increase retention of migrators in biological hotspots (Carr, 2003, 2006; Emsley et al., 2005; Lavoie et al., 2000). In the Gulf of St. Laurence, euphausiid species can perform DVM between two different flow fields in the Laurentian Channel, which result in accumulation inshore (Lavoie et al., 2000). Deep sills in the channel also help concentrate and prevent the flushing of krill at depth (Lavoie et al., 2000). Simulated particles in a two-layer system within Monterey Bay suggests that particles performing DVM are retained within the region, allowing juvenile euphausiids and other zooplankton to be retained within this hotspot (Carr, 2003, 2006). In the Irish Sea, the presence of DVM in simulated particles increased the probability of retention within the region up to 37% after 90 days due to the presence of a subsurface eddy (Emsley et al., 2005). Recent modeling work in the same region, however, suggests that DVM behavior may reduce residence times in these regions of the West Irish Sea, with the addition of DVM behaviors in their model halving the percentage of retained particles (McGeady et al., 2019). They hypothesized that DVM reduced retention times by reducing the amount of time spent at depths where eddy circulation is strongest (McGeady et al., 2019).

For zooplankton performing DVM, time spent within these potentially retentive features will be the ultimate driver of retention times. Since DL, defined here as the number of hours the sun is above the horizon, is one of the major modulators of DVM and the time spent at depth in retentive flows, DL may have a significant impact on retention times for organisms performing DVM. DL has a significant impact on DVM behavior in high latitudes where seasonal variability in DL is greatest (Benoit et al., 2010; Cohen & Forward, 2005; Conroy et al., 2020; Hobbs et al., 2018). Long days may decrease the distance of DVM behavior, or stop it completely at high latitudes when days are longest (Cisewski et al., 2010; Conroy et al., 2020).

Another potential modulator of retention times in subsurface features is mixed layer depth (MLD). When stratification is high, the surface mixed layer can be distinct from the rest of the water column, and driven by different forcing mechanisms than the waters below the MLD (Johnston & Rudnick, 2009). Flow in the upper mixed layer, for example, may be more driven by wind or freshwater inputs, while flow below the MLD may be driven by bathymetry. The current velocities and directions between these two layers can differ significantly (Kohut et al., 2018). The MLD is often used as a proxy depth for the boundary between these layers. Given the large differences in current velocity between the two layers, theoretically, there would be

benefits to migrating out of the variably forced surface mixed layer and into a slower-moving, more steady, subsurface layer. Shallower mixed layers may help increase retention of migrating zooplankton by reducing the vertical distance required needed to reach the quiescent or recirculating subsurface, and increasing the time spent at these depths. While previous studies have suggested that both MLD and DL affect zooplankton DVM distances and the occurance, the effects of these factors on retention of zooplankton performing DVM is relatively unknown.

Palmer Deep Canyon (PDC) is a deep, nearshore, submarine canyon along the West Antarctic Peninsula (WAP) (Carvalho et al., 2016; Fraser & Trivelpiece, 1996; Kavanaugh et al., 2015; Schofield et al., 2013). It is considered a biological hotspot due to its proximity to Adélie and gentoo colonies and foraging regions, as well as high whale foraging activity (Fraser & Trivelpiece, 1996; Schofield et al., 2013). These predators feed on a variety of zooplankton that perform DVM behaviors including euphausiids, such as the Antarctic krill (*Euphausia superba*), several calanoid copepod species, and ostracods (Conroy et al., 2020; Demer & Hewitt, 1995; Thibodeau, 2015). The extent of zooplankton migrations throughout the WAP is highly variable by season and latitude, with DVM being more prevalent in the northern WAP during the summer (Cleary et al., 2016; Conroy et al., 2020; Thibodeau, 2015). DL and MLD have been shown to influence DVM along the WAP (Conroy et al., 2020). Ostracods and other zooplankton perform shallower DVMs when days are long and mixed layers are deeper than 50 m (Conroy et al., 2020).

Recent *in-situ* and modeled observations of PDC show that a closed, subsurface eddy is present within PDC during the austral summer when biological activity is high (Supplemental Movie 1; Hudson et al., 2019, 2021). The subsurface eddy increases residence times of neutrally buoyant particles up to 175 days at 150 m depth in comparison to 2-4 days in the surface (Hudson et al., 2021). Models suggest that flow is mostly barotropic, with a small baroclinic component (Hudson et al., 2021). *In-situ* observations of isopycnal doming over the canyon suggest that the baroclinic component to the flow is greater than the model predicts (Hudson et al., 2021). The baroclinic component of the flow is believed to dominate below the MLD, with isopycnal doming present as shallow as 75 m over the deepest portions of the canyon (Hudson et al., 2021).

We test the hypothesis that the subsurface eddy present within PDC increases the residence time of vertically migrating zooplankton within this biological hotspot. We also test

142 the hypothesis that the depth of the boundary between the surface mixed layer and subsurface
143 eddy, approximated by MLD, and DL significantly impact these residence times. We also
144 hypothesize that vertical migration in this subsurface feature increases residence times and that
145 shallower MLDs and longer days will increases residence times in the system. If DVM is both
146 present within PDC and facilitates the retention of zooplankton within the canyon system, this
147 mechanism could provide a reliable food resource for higher trophic levels, and facilitate the

148 formation of a biological hotspot.

149

2 Materials and Methods

2.1 Observations of DVM in PDC

2.1.1 Mooring Observations

A mooring was deployed within PDC during the austral summer of 2020 to help visualize the extent of DVM within PDC (Figure 1b). It was equipped with a Nortek Signature 100 equipped with an echosounder. It was deployed on 6 January 2020 to 345 m depth and recovered on 3 February 2020. The echosounder pinged at 3 s intervals and had a frequency sweep from 70 - 120 kHz. Only the 120 KHz frequency was examined here.

2.1.2 Krill Swarm Identification from Glider-Based Acoustics

To visualize the extent of krill swarm DVM within PDC, we utilized two Slocum electric glider deployments conducted during the austral summer of 2020 (Figure 1b). The two gliders used in this analysis were deployed on 9 January 2020. One was recovered on 21 February 2020 and the other was recovered on 11 March 2020. These gliders occupied two primary transects: a transect moving across the canyon, parallel to the coast near the head of the canyon and a perpendicular transect moving along the long axis of PDC (Figure 1b). The along-canyon glider also opportunistically sampled two additional transects: a deep-across canyon transect, parallel to the across-canyon transect but over the deepest portions of the canyon; and a shelf-canyon line, moving from the end of the along-canyon transect, over the sill of the canyon, and onto the continental shelf (Figure 1b). The across-canyon glider sampled down to 200 m and the glider that primarily sampled on the along-canyon transect sampled down to 1000 m.

The gliders were equipped with an Imaginex853 single-beam (120 kHz) echosounder. Acoustics were sampled only on down casts. Raw returns were converted to mean volume backscattering strength (S_v) using the following equation (Guihen et al., 2014):

$$(1)\; S_v = RBV + 20\log_{10} R + 2\alpha R - (RR + SL) - \left(10\log_{10}\frac{c\tau}{2}\right) - (10\log_{10} EBA) - C - g$$

Where RBV is the recorded count ($20\log_{10}[signal\,level]$¿; RR and SL were transducer receiving response (dB re $\frac{1\,V}{\mu Pa}$) and transducer source level (dB re 1 μPa at 1 m), respectively, supplied by the manufacturer for each echosounder; α is absorption coefficient (dB m^{-1}); c is sound

177 velocity (m s^{-1}); τ is pulse length (s); EBA is the equivalent beam angle (steradians); g is gain
178 (dB); and C is a constant calculated during echosounder calibration.
179 Both echosounders were calibrated in July 2019 at the National Ocean and Atmospheric
180 Administration's (NOAA) Southwest Fisheries Science Center (SWFSC). Absorption
181 coefficient, sound velocity, pulse length, and equivalent beam angles were kept constant between
182 the two instruments since they were calibrated in the same conditions. Range and gain were kept
183 constant (100 m and 40 dB, respectively) between the two instruments. Both instruments were
184 programmed to sample in 'glider' mode: one ping every 4 seconds.
185 After converting raw returns to S_v, bin depths were corrected using the pitch of the glider
186 using the following equation:
187 $$(2)\ CorrectedBinDepth = (BinNumber * 0.5) * \cos(gliderPitch - 22) + gliderDepth$$
188 Where BinNumber is the bin number provided by the echosounder and is multiplied by 0.5 to
189 convert the raw number to half meter bins; and gliderPitch (converted from radians to degrees)
190 and gliderDepth (m) are the pitch and depth reported by the glider, respectively. This correction
191 was done to account for any difference in the glider pitch and echosounder angle that would
192 result in the echosounder not being parallel to the bottom.
193 Krill swarms were identified within the glider acoustic data and used to determine if krill
194 were performing DVM in this region. Krill swarms were counted by plotting individual acoustic
195 profiles from the glider-mounted Imaginex853 instruments. Krill swarms were plotted and
196 annotated using an RShiny application, which allowed the user to highlight each krill swarm and
197 save the corresponding glider timestamps and bin depths from each krill swarm (Figure S1). The
198 app allowed users to customize plots by time, length of time to plot, number of bins to exclude
199 from plotting to reduce noise, dB thresholds, and platform (Figure S1). The saved csv files were
200 then compiled and matched to the complete glider dataset to determine the presence-absence of
201 krill swarms. The code used to produce the RShiny application, along with example data and
202 app, are available online (Hudson, 2021).
203 The *sunangle* function in the R package *oce* (Kelley & Richards, 2020; R Core Team,
204 2020) was used to determine if krill swarms occurred during daytime and nighttime hours, with
205 daytime being classified as having a sun angle greater than 0. Median swarm depth and sun angle
206 were used to determine the prevalence of DVM. The depths of krill swarms observed during the
207 day versus night were compared with a Wilcoxon Rank Sum test.

208 ### 2.2 Diel Vertical Migrations and Residence Time Calculations in ROMS

209 The Regional Ocean Modeling System (ROMS) (Haidvogel et al., 2008) was used to test
210 the impacts of DVM on particle residence times within PDC. The updated (Hudson et al., 2021)
211 WAP version of ROMS (Graham et al., 2016) has a 1.5 km horizontal resolution with 24 terrain
212 following vertical layers. It includes modeling of dynamic sea ice (Budgell, 2005) and the
213 interactions between floating ice shelves and the water beneath them (Dinniman et al., 2011;
214 Holland & Jenkins, 1999). Atmospheric forcing is from the Antarctic Mesoscale Prediction
215 System (Powers et al., 2012) and tidal forcing is from the CATS2008 regional Antarctic tidal
216 model (Padman et al., 2002). Simulations were run from November 2008 to May 2009.
217 Neutrally buoyant particles were released on an approximately 4 km grid around PDC
218 every 2 days (Figure 1a) from the beginning of the run through the end of March 2009. Particles
219 were advected within the model code at every model time step (50 s) and included a vertical
220 random walk (Hunter et al., 1993; Visser, 1997) to mimic the transport effect of vertical
221 turbulence (which is parameterized in the model). Particles positions were saved every hour.
222 DVM behavior was added to the particles based on the local solar angle (Figure 2). If the sun
223 was above the horizon at the position of the particle, then a downward velocity was added to the
224 advective and random vertical velocities as long as the particle was above some maximum depth.
225 If the sun was below the horizon, then an upward velocity was added as long as the particle was
226 below some minimum depth.

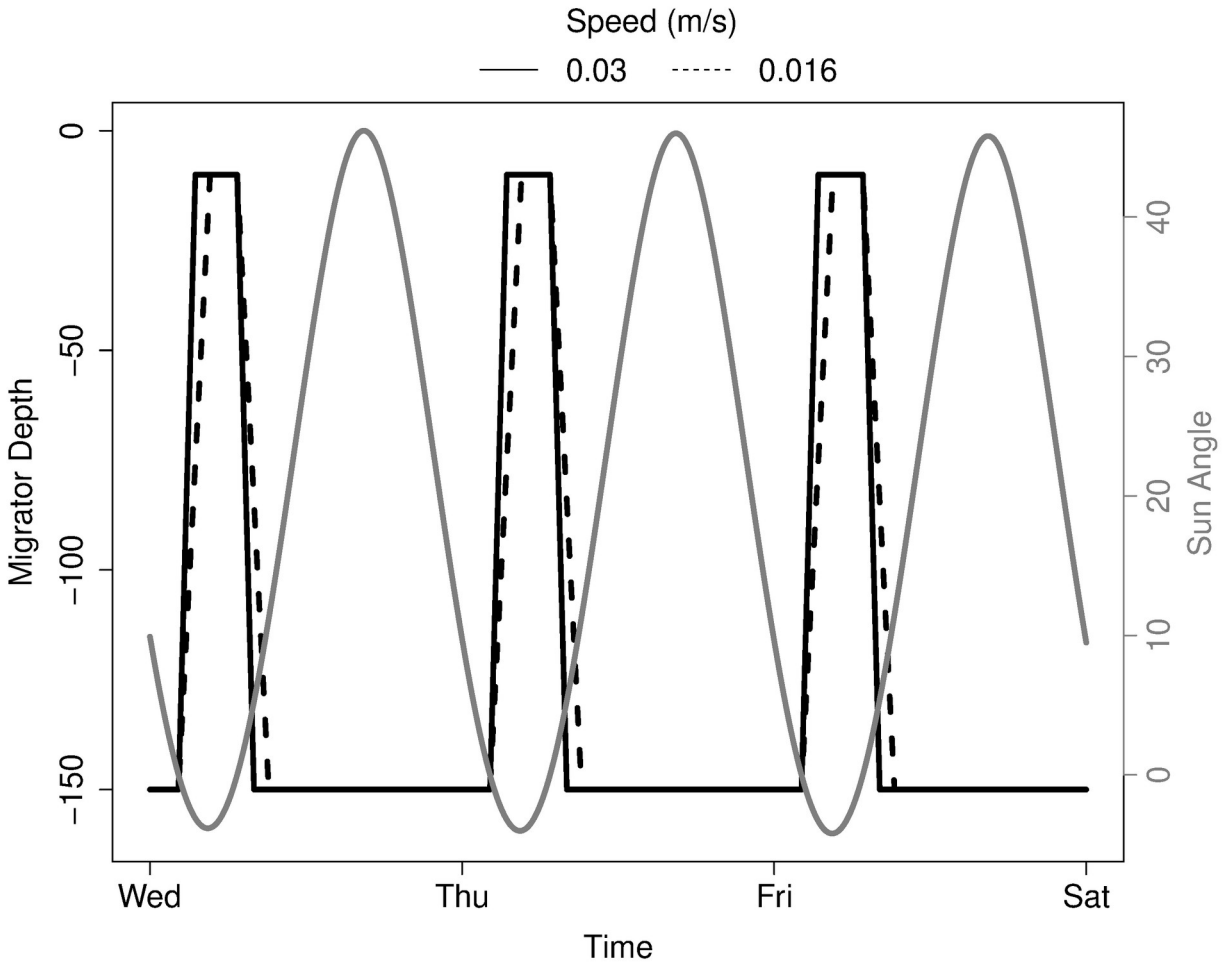

Figure 2. Idealized diel vertical migration in simulated particles within PDC over a four-day period in early January 2020 as cued by sun angle (left y-axis) at the two different swimming speeds used in this study. Time is local to PDC. Note that this figure illustrates an idealized example of DVM and does not include the vertical advective velocity or random walk that is an option in ROMS.

Migration depths were based on *in-situ* observations (Figures 2-3) and idealized simulations (Figures S2-4; Supplementary Text 1). To ensure particles migrated out of the mixed layer, we set our shallowest depth migration to 50 m. We also simulated migration down to 150 m as an intermediate between 50 and 300 m.

Migration speeds were based on *in-situ* observations (Figure 2), idealized simulations (Figures S2-4; Supplementary Text 1), and previously published vertical swimming speeds of krill (Kane et al., 2018; Kils, 1981). Mean vertical swimming speeds of krill in the late spring were reported as approximately 0.23 body lengths per second (Kane et al., 2018). We used a mean body length estimate of 5 cm to calculate a swimming speed of 0.016 m s^{-1}. We also

calculated a vertical swimming speed of acoustic scatterers observed in mooring data of 0.03 m s^{-1}, which was similar to previously published vertical swimming speeds (Kils, 1981; Figure S2).

Based on these observations and simulations, particles migrated between 10-50, 10-150, and 10-300 m at 0.016 m s^{-1} and 0.03 m s^{-1}. Neutrally buoyant particles were also simulated without DVM behavior at 10, 50, 150, and 300 m. For all simulations, all particles were passive drifters with the 3d current other than DVM behavior and modeled vertical diffusion. No active swimming against or with currents were considered.

Residence times were calculated using the e-folding method, defined as the time needed for the concentration of particles to drop to 1/e (~37%) (Couto et al., 2017; Kohut et al., 2018; Piñones et al., 2013). Residence times were calculated for particles released over PDC, using both particle position and the 400 m isobath to define PDC (Figure 1a). Residence times were calculated for the period between 21 December 2008 and 21 February 2009 when the subsurface eddy was most coherent over PDC based on daily averaged currents (Supplemental Movie 1). The residence times were compared using a Kruskal-Wallis test with Dunn's post-hoc test with Bonferroni correction. Migrating particles at both speeds were compared to the 10 m particle release to test if migrating significantly changed residence times in comparison to the surface. Residence times of particles without migrating behavior were also compared in separate Kruskal-Wallis and post-hoc tests.

DL was calculated in hours from ROMS. MLD was calculated using the depth of maximum Brunt-Väisälä frequency (N^2) (Carvalho et al., 2017). DL and MLD were averaged over the calculated residence time (from particle release to the time where particle concentration drops to ~37%) for each particle release. The effect of these values on residence times of migrating particles was compared using a Weighted Least Squares (WLS) multiple regression without interaction of MLD and DL. WLS was used, and the interaction was not considered, to control for homoscedasticity in the data and collinearity of MLD and daylength, respectively. Homoscedasticity was tested using *ncvTest* in the *car* package in R (Fox & Weisberg, 2019). Variance Inflation Factors (VIF) were calculated using *vif* in the car package (Fox & Weisberg, 2019). VIFs for the final models ranged between 1.58 and 2.74. Weights (*w*) were generated using the following equations:

(3) $$mod1 = lm(RT \quad meanMLD + meanDL)$$

(4) $$fitted.values = lm(|mod1\$residuals| \quad mod\$fitted.values)\$fitted.values$$

(5) $$w = \frac{1}{fitted.values^2}$$

Outliers were detected using the *outlierTest* function in the *car* package (Fox & Weisberg, 2019). A total of two outliers were removed from particles migrating between 10-300 m, one from each migrating speed, to help meet model normality assumptions, which was tested using a Shapiro-Wilk test in the *stats* package (R Core Team, 2020).

3 Results

3.1 Diel Vertical Migration in Palmer Deep Canyon

The subsurface mooring directly observed DVM behavior in local zooplankton populations (Figure S2). Scatterers in the top 50 m migrated to depths as great as 300 m, where layers of scatterers were greater than 50 m thick during the day (Figure S2). These migrations took approximately 2 hours, meaning that scatters were migrating at approximately 0.03 m s^{-1} (Figure S2).

We identified 275 krill swarms with 197 observed on the across-canyon transect and the remaining 78 swarms observed on the along-canyon transect (Figure 3). No krill swarms were observed on the deep-across or shelf-canyon transects. Of these, 218 were observed during the day and 57 were observed at night. The median depth of krill swarms observed during the day was 11.75 m with an interquartile range between 6.68 m and 25.83 m (Figure 3). The median krill swarm depth increased to 9.14 m at night, with an interquartile range between 6.00 m and 13.15 m (Figure 3). While these migrations differed by approximately two meters, these depths were significantly different from each other ($p = 0.005$). This small, but significant difference could have been driven by a myriad of factors, including dilute krill populations in the region that were not able to be detected with manual annotation of the Imaginex853 data (see Section 4.1). No krill swarms were observed below 150 m and most swarms were observed above 50 m, even during the day (Figure 3). The max depth of krill swarms observed during the day was approximately 120 m while the max depth of krill swarms observed at night was 50 m (Figure 3).

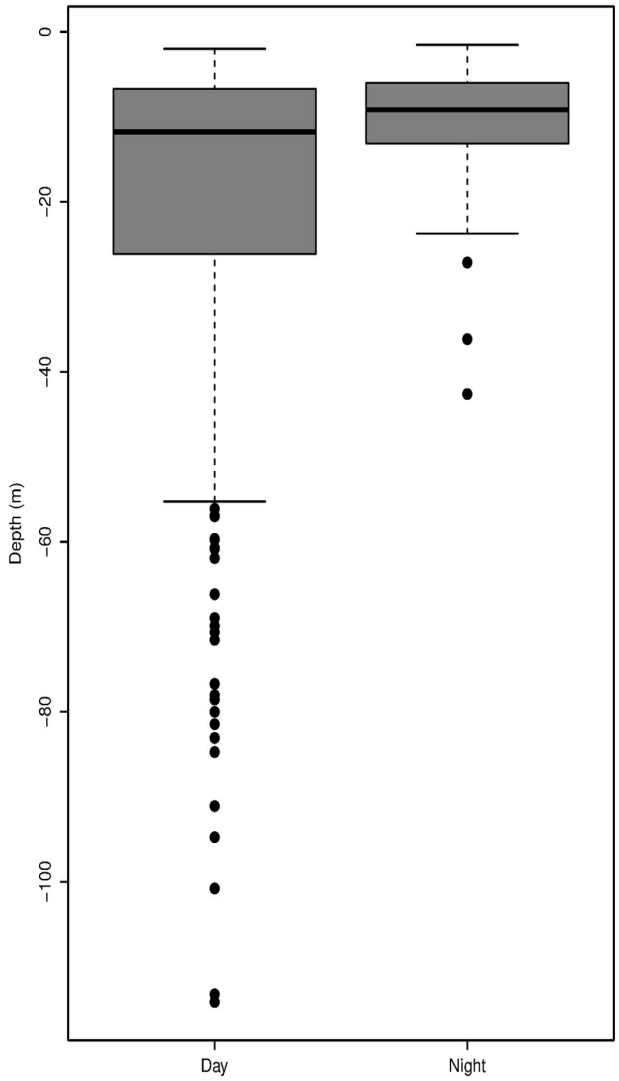

Figure 3. Barplot illustrating the number of krill swarms observed during daylight and nighttime hours by the single channel echosounders deployed on the two gliders used in this analysis.

293

294 3.2 Effect of Diel Vertical Migration on Residence Times

295 The residence time of non-migrating particles increased at deeper depths (Figure 4a).
296 Particles released at 10 m depth had a median (± 95% confidence interval) residence time of 6.96
297 (± 0.27) days, which is significantly shorter than deeper residence times. Particles released at 50
298 m depth, which had a median residence time of 25.00 (± 0.48) days, had significantly different
299 residence times from particles released at depths of 10, 150, and 300 m ($p \leq 0.003$, Figure 4a).
300 Particles released at 150 and 300 m depth had residence times of 197.71 (± 2.60) and 127.24 (±

1.35) days (Figure 4a), respectively. They did not statistically differ from each other ($p = 1$) but residence times at 150 and 300 m depth differed from residence times at 10 and 50 m depth ($p << 0.001$; Figure 4a).

As particles migrated deeper, residence times increased significantly in comparison to non-migrating particles released at 10 m (Table 1). While residence times at both speeds were significantly different from non-migrating particles, there was no significant difference in residence times between the two swimming speeds ($p = 0.86$). Particles migrating between 10 and 50 m depth had median residence times ~ 68 % greater than residence times at 10 m depth (Figure 4b; Table 1), however, they were not statistically different from residence times at 10 m ($0.06 < p < 0.11$). Particles migrating to 150 m had median residence times 194.61 – 268.86% greater than residence times at 10 m depth (Figure 4b; Table 1). Particles migrating to 150 m had significantly greater residence times than non-migrating particles released at 10 m ($p << 0.001$). Particles migrating between 10 and 300 m depth had residence times 288.62 – 385.03% greater than residence times at 10 m depth (Figure 4b; Table 1). These residence times were significantly different from median residence time at 10 m ($p << 0.001$). Particles migrating down to 150 and 300 m depth did not have significantly different residence times ($0.24 < p < 0.81$; Figure 4b).

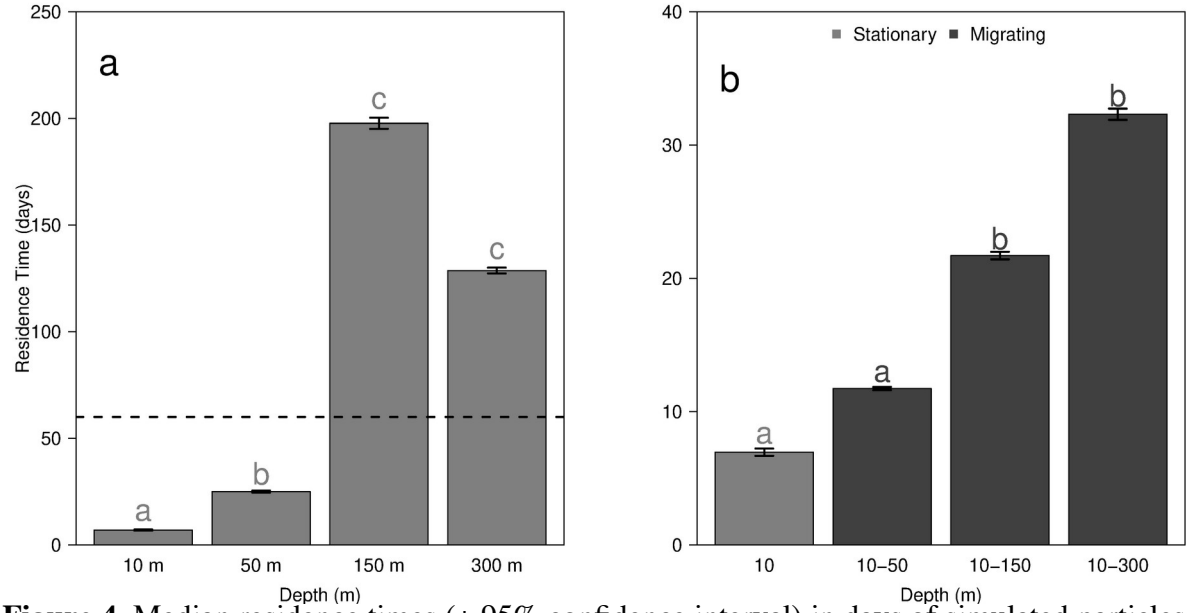

Figure 4. Median residence times (± 95% confidence interval) in days of simulated particles released without diel vertical migration behavior (a) and with vertical migration behavior at three different migration depths (b). Swimming speeds were pooled because there was no statistical difference between the two migration speeds. The horizontal dashed line in panel a represents a residence time of 60 days, the approximate length of peak biological activity in the system. The same letters above the bars in each panel indicate which of the four separate populations are statistically similar as determined by Kruskal-Wallis tests and Dunn's post-hoc tests with Bonferroni corrections.

317

Vertical Swimming Speed (m s^{-1})	Migration Depth (m)	Median Migrating Residence Time (days) ± 95% Confidence Interval	Percent Change from Median Residence Time at 10 m (%)
0.016	50	11.71 (± 0.24)	+68.27
0.016	150	25.67 (± 0.58)	**+268.86**
0.016	300	33.75 (± 0.85)	**+385.03**
0.03	50	11.75 (± 0.27)	+68.86
0.03	150	20.50 (± 0.55)	**+194.61**
0.03	300	27.04 (± 0.80)	**+288.62**

Table 1. Residence times of migrating and non-migrating particles across the migration depths, and their differences, in the subsurface eddy in Palmer Deep Canyon. Bolded values indicate that the differences between the residence time of migrating particles was significantly different from the corresponding non-migrating particles, as determined by Kruskal-Wallis tests and Dunn's post-hoc tests with Bonferroni correction.

MLD over PDC averaged 36 m over the study period (21 December 2008 and 21 February 2009) (Figure 5a). MLD decreased from approximately 55 m to nearly 20 m in early January (Figure 5a). It periodically shallowed and then gradually deepened over the course of the study period, with MLD becoming as shallow as 5 m in the second week of January and 10 m at the end of January (Figure 5a). The MLD was approximately 30 m through February (Figure 5a). DL decreased from 21 to nearly 15 hours over the course of the study period (Figure 5a). The rate of this change increased into February (Figure 5a).

Residence times for particles migrating to 150 and 300 m declined gradually at both swimming speeds over the study period (late December 2008 – late February 2009) (Figure 5b-c). For late December releases, residence times ranged between 40 – 68 days for particles migrating to 300 m and ~30 days for particles migrating to 150 m for both swimming speeds (Figure 5b-c). This gradually declined to ~10-15 days for both swimming speeds and both migration depths for releases in the second week of February (Figure 5b-c). Residence times for released particles migrating to 50 m were relatively stable at ~15 days until this time period, after which they also started to decline (Figure 5b-c). Residence times of non-migrating particles

334 released at 10 m were highly variable, ranging between 5 and 20 days (Figure 5b-c). There were
335 releases in late December to early January and early February where these residence times were
336 much lower than the residence times of particles migrating to 50 m at both swimming speeds.
337 There were also releases where these residence times were nearly identical throughout January
338 (Figure 5b-c).

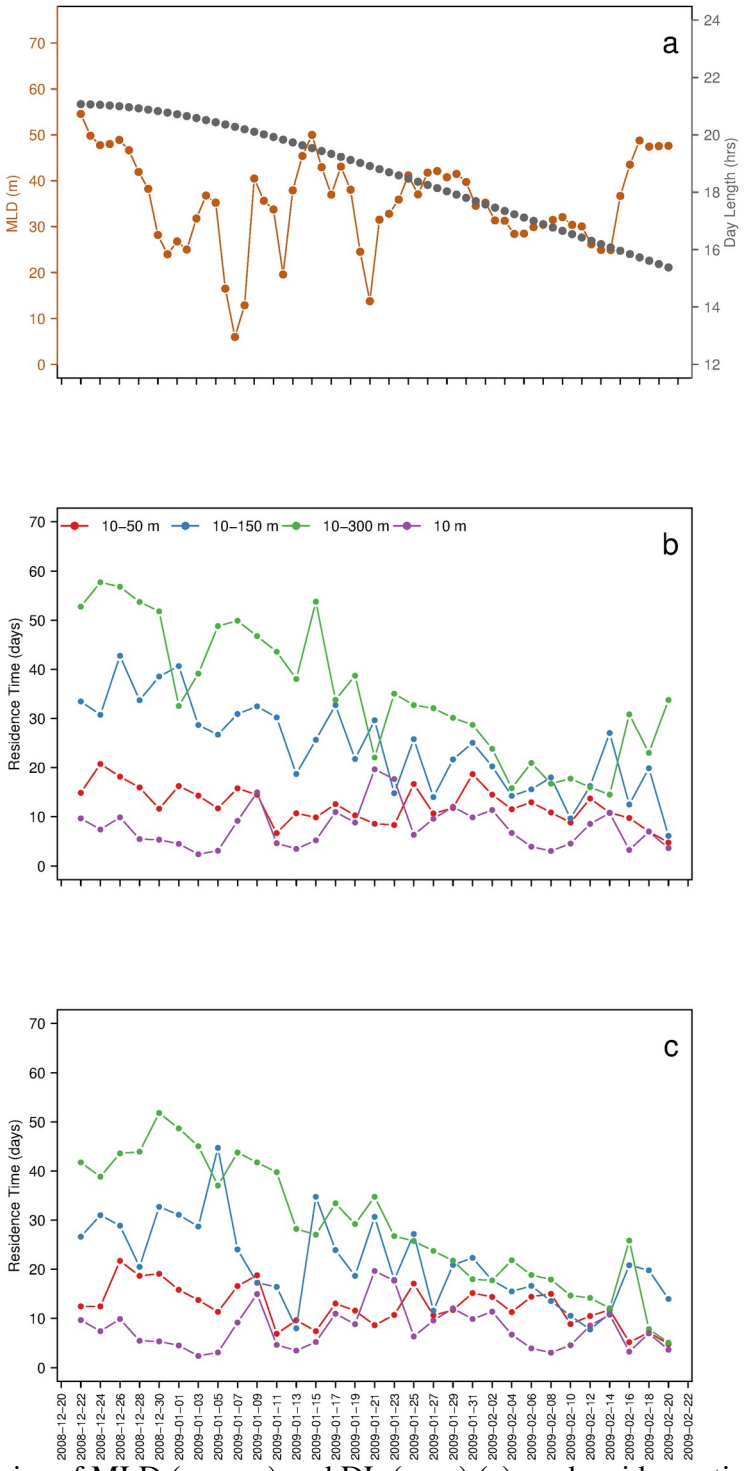

Figure 5. Time series of MLD (orange) and DL (grey) (a); and residence times of migrating particles at 0.016 m s^{-1} (b) and 0.03 m s^{-1} (c) compared to residence times of non-migrating particles released at 10 m when the subsurface eddy is most coherent in the austral summer.

339

340 ### 3.3 Effect of MLD and DL on Residence Times

341 For particles migrating between 10 and 50 m, deepening mixed layers decreased the
342 residence times (Figure 6a). For each meter that the MLD deepened, the residence times
343 decreased by approximately half a day (Table 2). MLD has a significant effect on residence
344 times ($p < 0.001$; Table 2). While residence times increased as days grew longer, DL did not
345 have a significant effect on residence times for particles migrating between 10 and 50 m (Figure
346 6a; $p = 0.1$; Table 2). The overall model was significant ($p << 0.001$; Table 2) and explained
347 nearly half of the variance observed ($R^2 = 0.48$; Table 2).
348 For particles migrating between 10 and 150 m, MLD had no significant effect on
349 residence times ($p = 0.07$; Table 2). Residence times for these particles significantly increased
350 with DL ($p = 0.002$; Figure 6b; Table 2). For each additional hour of daylight, residence times
351 increased by 2.43 days (Table 2). The model was significant ($p < 0.001$) and explained a third of
352 the variance ($R^2 = 0.33$; Table 2).
353 For particles migrating between 10 and 300 m, both DVM and DL had significant effects
354 on the residence times ($p < 0.001$; Figure 6c; Table 2). Deepening MLD had reduced particle
355 residence times, while increasing DL increased residence times (Figure 6c; note two overlaying
356 points in red were considered outliers and not included in the WLS; Table 2). Residence times
357 decreased by 0.57 days for every meter MLD deepened and increased by 8.33 days for every
358 hour DL increased (Table 2; Figure 6c). Together, these variables explained nearly all the
359 variance present ($R^2 = 0.94$; Table 2). The model was highly significant ($p << 0.001$; Table 2).

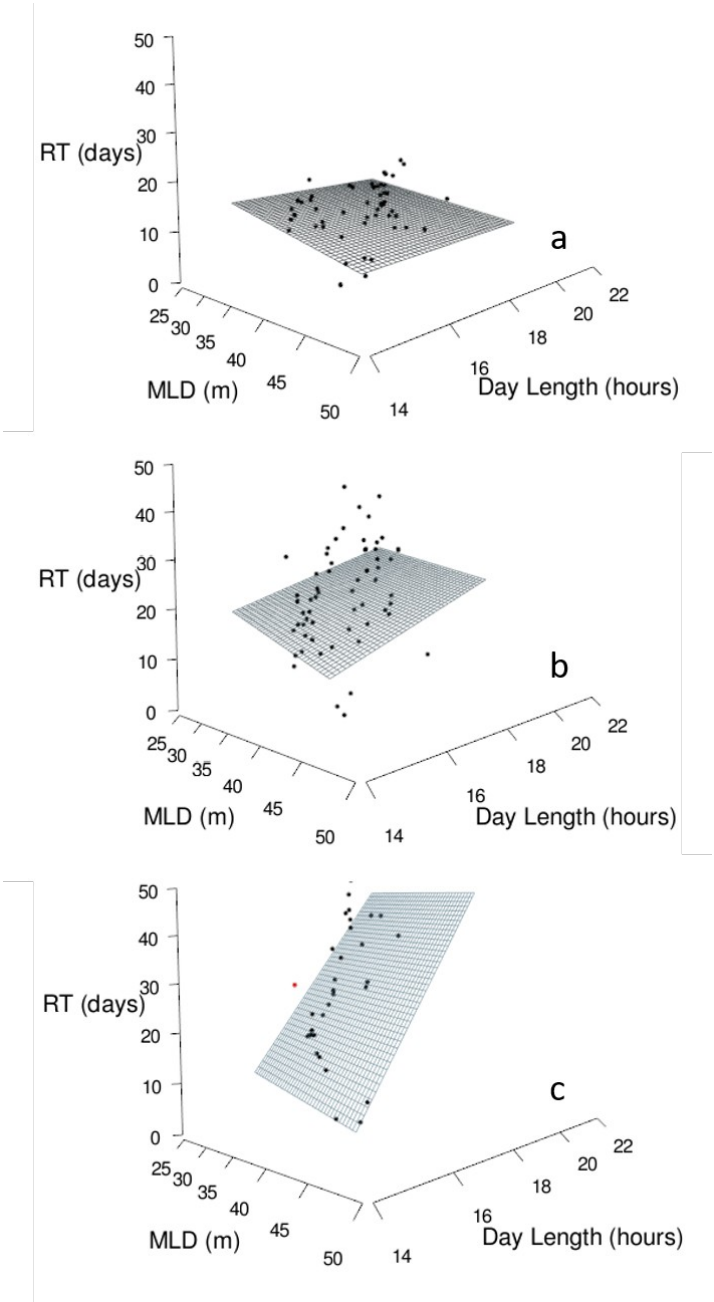

Figure 6. WLS regressions of residence times (RT) as a function of mean MLD (m) and mean DL (hours) for particles migrating between 10-50 m (a), 10-150 m (b), and 10-300 m (c) at both 0.03 m s^{-1} and 0.016 m s^{-1}. Planes are generated from WLS predictions. Red points indicate outliers that were not included in WLS regressions.

360

Migration (m)	Model Terms	Slope	Standard Error	t-value	p	Model R^2	Model p
10-50	MLD (m)	-0.52	0.10	-4.95	**$6.59 * 10^{-6}$**	0.48	**$1.26 * 10^{-9}$**
	DL (hrs)	0.46	0.28	1.67	0.10		
10-150	MLD (m)	-0.74	0.40	-1.85	0.07	0.33	**$2.32 * 10^{-6}$**
	DL (hrs)	2.43	0.77	3.17	**0.002**		
10-300	MLD (m)	-0.57	0.13	-4.50	**$3.43 * 10^{-5}$**	0.94	**$< 2.2 * 10^{-16}$**
	DL (hrs)	8.33	0.60	13.94	**$< 2.2 * 10^{-16}$**		

Table 2. Results from WLS regressions on the effect of MLD and DL on the residence times (in days) of simulated particles migrating to three depths. Migration speed was not considered in these models. Two outliers were removed from particles migrating between 10-300 m for regressions (see Figure 6).

4 Discussion

Biological hotspots serve several roles for the organisms that utilize them (Hazen et al., 2013). They can be important life history areas for species like central place foragers who rely on the resources around them while raising their offspring (Hazen et al., 2013 and sources therein). They can also be regions of high biodiversity and abundance or areas of high productivity, bio-physical coupling, and trophic transfer (Hazen et al., 2013 and sources therein). Understanding the mechanisms that drive these critical areas will not only help make management decisions about these areas and the organisms they support, but also understand how they will shift under future climate change scenarios (Hazen et al., 2013).

One such biological hotspot exists around PDC. This region is a critical foraging grounds for surrounding penguin colonies and transient whale populations during the austral summer (Schofield et al., 2013). The region is also very productive in the austral summer, attracting many prey species for these foragers (Carvalho et al., 2016; Kavanaugh et al., 2015). The

presence of PDC near the hotspot has long been hypothesized to facilitate the unique physical and biological processes that drive the hotspot (Fraser & Trivelpiece, 1996; Schofield et al., 2013). Glider and satellite observations from PDC and the surrounding area suggested that the upwelling of warm, nutrient-rich subsurface water was responsible for driving the increased production in the area (Kavanaugh et al., 2015; Schofield et al., 2013). However, a lack of seasonal upwelling in long-term observations (Carvalho et al., 2016; Hudson et al., 2019), low surface residence times (Kohut et al., 2018), and a lack of physiological response in surface phytoplankton populations to this nutrient-rich water (Carvalho et al., 2020) suggest that upwelling is likely not driving this hotspot.

Observations of isopycnal doming within the canyon suggested that a subsurface recirculating feature may be present within the canyon (Hudson et al., 2019). ROMS simulations and the persistence of the isopycnal doming across multiple field seasons suggest that there is a recirculating, subsurface eddy over PDC in the austral summer (Supplemental Movie 1; Hudson et al., 2021). Simulated particle releases in this feature suggest that residence times increase significantly below the mixed layer, with median residence times as high as 175 days at 150 m during the austral summer (Hudson et al., 2021). If zooplankton populations, which are a critical food source within PDC, are performing DVM, they are most likely interacting with this subsurface feature, which could facilitate retention within and near the hotspot.

We tested the hypothesis that DVM would increase particle residence times over PDC due to the presence of this subsurface eddy. We also tested the impacts of the depth of the boundary between the surface mixed layer and subsurface eddy, proxied by MLD, and DL on these residence times. MLD impacts the current fields experienced by particles at the surface and the distance needed to travel to reach the subsurface retentive layer. DL modulates the frequency and timing of DVM behaviors. Both factors can also change the amount of time particles interact with the subsurface eddy. We hypothesize that performing DVM increases particle residence times, relative to surface residence times, and that shallower MLDs and longer days would increase residence times by increasing the time spent within this subsurface feature.

4.1 DVM Observations

Echosounder observations on two gliders and a subsurface mooring deployed in 2020

illustrated the extent of DVM present in zooplankton populations in and around PDC (Figure 2-3). The subsurface mooring deployed observed regular DVM behavior down to 300 m with scatters migrating at approximately 0.03 m s^{-1} (Figure S2). Glider-based, downward facing echosounders observed significantly different mean depths in the 275 krill swarms observed during the daytime and nighttime (Figure 3). Krill swarms were observed between 6.68 m and 25.83 m during the day and between 6.00 m and 13.15 m at night (Figure 3). While the median depth of the swarms at day and night were statistically different, the magnitude of the migration is much smaller than migrations observed previously by similar platforms (Goodrich, 2018). In 2015, krill swarms within PDC were observed at approximately 20 m at night and between 40 and 80 m during the day using an upward looking Acoustic Doppler Current Profiler (ADCP) on a Slocum glider. These are deeper than our observations using a downward looking Imaginex853 echosounder on a similar vehicle.

There was also a significant difference in the extent of DVM behavior between the glider-based and subsurface mooring observations. One possible explanation for this discrepancy is the different methodologies used between the two platforms. Only krill swarms were identified in the glider-based acoustics while all scatterers were considered in the mooring data. This was done in part due to the different resolutions of the two instruments. The echosounder on the Nortek Signature 100 has a much higher resolution than the Imaginex853 deployed on the gliders. Another possible explanation for this discrepancy is the spatial and temporal resolutions of the two platforms. The mooring was stationary while the gliders moved throughout the study region. As a result, the differences in DVM behavior in the glider observations may have been the result of spatial and temporal smearing. Krill were extremely patchy in 2020 near PDC (M. Oliver, personal observation), therefore could have been easily missed while the glider transited.

The differences in the DVM observations described here are not uncommon. Many studies differ on the extent of krill DVM observed throughout the Southern Ocean (Tarling et al., 2018 and sources therein). One difference that could have caused this change between the 2015 and 2020 field campaigns was the difference in productivity within PDC in the two field campaigns. Surface chlorophyll concentrations and optical backscatter measured by the Slocum gliders in 2015 were much higher, especially earlier in the summer, in comparison to 2020 (Hudson et al., 2021). Krill swarms observed in 2020 may have been higher in the water column to search for these restricted food sources. There were also more salps observed in 2020 than in

2015 (M. Oliver, personal observation), which may have impacted the vertical distribution of the krill within PDC. In addition, krill may have been highly dispersed within the water column, instead of forming tight swarms, making swarms hard or impossible to detect manually with the Imaginex853. Krill can form denser swarms during the day versus more dilute concentrations at night, which could help explain why nearly 72% of krill swarms identified were observed during the day (Brinton & Antezana, 1984; Everson, 1983). Therefore, it is possible that these more dilute krill could have been missed by the acoustic sensors utilized in this study.

4.2 Effect of DVM on Residence Time

DVM observations were used to parameterize migration depths and swimming speeds in ROMS simulations. Residence times of non-migrating, non-vertically migrating particles generally increases with deeper depths within the canyon, with the highest residence times of 197.71 (± 2.60) days observed at 150 m (Figure 4a). Here, we show similar trends in vertically migrating particles. Residence times increase at the deeper migration depths with the highest residence times observed in particles that migrate between 10 and 300 m depth (Figure 4b). We examined two swimming speeds, based on thresholding experiments and previously published vertical swimming speeds, and found that there was no significant effect of the two tested swimming speeds on residence times. The depth of the migration had the biggest effect on residence times over the depths tested (50, 150, and 300 m) (Figure 4b; Table 1).

Particles migrating to the deepest depths had residence times 385% higher than residence times of non-migrating particles at 10 m (Table 1). While residence times of migrators swimming down to 150 and 300 m were statistically different from near surface residence times, migrations down to 50 m did not produce statistically different residence times from non-migrating particles at 10 m. Previous estimates of residence times of non-migrating particles suggest that residence times shallower than 50 m do not differ significantly from each other, but are statistically different from residence times deeper than 50 m (Hudson et al., 2021). Our results are similar, with particles migrating down to 50 m having statistically similar residence times to 10 m, but deeper migrations producing statistically different residence times (Figures 4b, 5; Table 1). The time series of residence times indicates that, while there are periods of time when migrators have residence times nearly twice that of non-migrating particles, there are also times where the residence times between migrating and non-migrating particles are nearly

identical (Figure 5). This would suggest that migration down to 50 m is statistically no different from staying at 10 m, especially at certain periods of the year, while migrating to deeper depths like 150 and 300 m, significantly increases the residence times of migrators.

4.3 Effect of MLD and DL on Residence Time

WLS regressions of the residence times of migrating particles suggest that they are strongly modulated by the depth of the boundary between the surface mixed layer and the subsurface retentive layer, proxied by MLD, and DL (Figure 6; Table 2). The relationship between MLD, DL, and particle residence times varied with depth. For particles migrating between 10 and 50 m, MLD had the biggest effect on residence times. For particles migrating to 150 m, DL had a significant effect on residence times. The residence times of particles that migrated down to 300 m were strongly influenced by both MLD and DL (Figure 6c; Table 2).

We used MLD to approximate the boundary between the two different flow fields present within PDC. Mean ROMS current velocities over PDC during the study period suggest that the current velocities at 10 m are faster and more variable than the waters below in PDC (Figure S4). The mean ROMS MLD was approximately 36 m (Figure 5a). Current velocities below 10 m were for the most part slower than currents at 10 m (Figure S5). Mean velocities at 300 m increased slightly on comparison to currents at 50 m and 150 m (Figure S5). We hypothesize that this is due to near-canyon rim effects at depth. Overall, these current velocities illustrate a rapidly moving, variable surface layer, and a slower moving, less variable, subsurface layer, support our hypothesis that there is a two-layer system present within PDC.

The significant influence of MLD on the residence times of particles migrating to 50 and 300 m depth suggests that migrating out of the rapidly moving surface layer is important to increasing residence times. Residence times were highest for migrating particles when the mean MLD experienced over their time in the canyon was shallower than 36 m, which was very similar to the mean MLD over PDC while the eddy was most coherent (35.36 m; Figures 5a, 6). This supported our hypothesis that a thinner surface layer, as indicated by shallower MLD would increase residence times. Importantly, ROMS may under predict MLD, and overall stratification in the PDC region (Figure S6; C. Moffat personal communication; Hudson et al., 2021). If the surface is more isolated from depth than the model predicts, migrating out of the mixed layer may increase residence times more than these simulations predict.

The importance of DL increases with depth, only having significant effects on residence times on particles migrating down to 150 and 300 m. WLS regressions suggest that for particles migrating to these depths, days with more than 18 hours of daylight result in residence times over 30 days and upwards of 50 days (Figure 6b-c). The significant effect of DL on residence times for deeper migrators did support our hypothesis that longer days would increase residence times. Longer days mean particles spend more time at depth, where residence times are higher than in surface waters (Hudson et al., 2021). Shorter days, and corresponding longer nights, would result in less time spent in the subsurface retentive layer and more time within the rapidly moving surface mixed layer where residence times are low (Hudson et al., 2021; Kohut et al., 2018), thus decreasing residence times.

We hypothesize that decreasing DL over the study period is the major driver of the decreasing residence times observed in particles migrating to these deeper depths where DL was a significant driver of particle residence times (Figures 5b-c; 6b-c). The WLS regressions suggest that decreasing DLs by one hour would decrease residence times by 2.43 and 8.33 days for particles migrating to 150 and 300 m, respectively (Table 2). Over the study period, DL decreases by approximately 6 hours (Figure 5a), which suggests that residence times for particles migrating to 150 and 300 m should decrease by approximately 15 and 50 days respectively. Residence times decreased on the same order of magnitude as the model predicts (Figure 5b-c) for particles with deeper migrations.

4.4 Limitations of our study

These simulations suggest that scatterers may be retained within the subsurface eddy over PDC through their DVM behavior, and that these residences times are driven by changes in MLD and DL. However, these model runs make many assumptions about zooplankton behavior. First, these simulations assume that zooplankton, especially krill, are passive drifters in the horizontal and only swim in the vertical. This is a common assumption in studies that model krill distribution (Cleary et al., 2016) and horizontal advection has been suggested as one of the major drivers of krill and other zooplankton distributions (Bernard & Steinberg, 2013; Bernard et al., 2017; Schofield et al., 2013). However, this ignores any predator avoidance or feeding behaviors that may affect distributions in the water column or migration distances.

524 The second assumption made in this analysis is that zooplankton are present at the depths
525 where simulated particles are released, and migration regularly occurs down to 300 m within
526 PDC. Zooplankton, including krill, have been observed as deep as 450 m and have been shown
527 to perform migrations down to 300 m in Wilhemina Bay near PDC (M. Amsler, personal
528 observation; Espinasse et al., 2012; Nowacek et al., 2011). Mooring acoustic returns suggest that
529 scatterers were present at and migrated to these depths, however, it is unclear if the observed
530 scatterers were zooplankton (Figure S2). In addition, while zooplankton can migrate to the
531 depths used in these simulations, they may choose not to complete the migration, based on a
532 variety of factors, including food and light availability. Individuals may also migrate deeper than
533 normal or sink before dawn due to increased predation pressure (Cresswell et al., 2009; Tarling
534 et al., 2002). *In-situ* observations of euphausiids suggested that krill may perform two migrations
535 during the night – one early in the night and another closer to dawn (Tarling & Johnson, 2006;
536 Tarling & Thorpe, 2017). Between these migrations, krill may swim or sink downwards while
537 they digest their meal, and then return to the surface just before dawn to feed again (Tarling &
538 Johnson, 2006; Tarling & Thorpe, 2017). This may not occur in the austral summer along the
539 WAP due to the short nights, especially at the peak of the austral summer. Observations along
540 the WAP suggest that some zooplankton decrease DVM behavior at the peak of the austral
541 summer (Conroy et al., 2020).

542 4.5 Implications for PDC and Beyond

543 Our study suggests that residence times of zooplankton performing DVM increase in
544 comparison to non-migrating scatterers in the near surface. This suggests that if zooplankton
545 perform DVM in PDC, they may be retained within the system for up to 35 days. WLS
546 regressions suggest that retention would be greatest if zooplankton migrated out of the surface
547 layer, where residence times are low (Kohut et al., 2018), and into the deep layer, where
548 residence times are highest (Figures 4, 6; Hudson et al., 2021). Retention would also be highest
549 when days are long enough to allow zooplankton to spend enough time at depth (Figure 6). The
550 boundary between the surface and deep layers is most likely modulated by the MLD, which
551 ranges between 10-50 m during the austral summer (Figure 6, S5; Hudson et al., 2019).
552 Migrations as deep as 80 m were previously observed in PDC (Goodrich, 2018), so migrations in
553 and out of this surface mixed layer may be possible, but more direct observations of DVM within

554 PDC are necessary to confirm the extent and variability of this behavior in local zooplankton
555 populations.

556 If zooplankton are retained within the subsurface eddy over PDC, they could provide a
557 reliable food source for nearby penguin colonies and transiting whale populations. Advection in
558 the surface layer could help transport zooplankton into the shallower, inshore regions where
559 these predators forage frequently and prevent them from completing their downward migration
560 that would put them out of reach of some foragers, depending on the depth of the migration. This
561 resource could prove critical to the hotspot, especially in low krill years like 2020, where
562 productivity is low and zooplankton may not be abundant, when the eddy may retain dilute
563 resources near the hotspot.

564 The timing of increased retention within the region aligns with local penguin foraging
565 behavior. Adélie penguins occupy PDC and the surrounding islands from late November to mid-
566 February. Foraging activity peaks after chicks hatch in early December and declines in early to
567 mid-February when the penguins leave the region following chick fledging (Ainley, 2002; Smith
568 et al., 1995). This corresponds to the increased residence times observed in December and
569 gradual decline into early February, which is likely a result of decreasing DL (Figure 5). This
570 suggests that migrators would have the greatest retention during this critical period for Adélie
571 penguins.

572 We have used PDC to examine how subsurface circulation features can increase the
573 residence times of organisms that perform DVM in and out of these features, but it is unlikely
574 that the processes described here are unique to this hotspot. Shallow surface mixed layers, as
575 proxied by MLD, and long days play a significant role in increasing residence times in this
576 feature but may control retention in other systems. While we have used an example of a closed,
577 recirculating subsurface eddy, the subsurface features that help increase retention of migrating
578 zooplankton or other organisms does not necessarily need to be a closed, recirculating feature.
579 Like in coastal upwelling regions, these features can be as simple as a return flow that is opposite
580 surface flows, thus reducing the net movement of migrators and retaining them within the system
581 (Peterson, 1998). The depths of these two layers – the surface mixed layer and the subsurface
582 layer – also will play a role, with shallower mixed layers increasing residence times of migrating
583 particles by decreasing the migration distance necessary to move into the retentive subsurface
584 layer. While DL was a significant driver of increased residence times at depth in our simulations,

585 this phenomenon may be unique to high latitudes where DLs are strongly variable and can
586 impact zooplankton DVM behavior (Conroy et al., 2020). The interaction of subsurface
587 circulation features, in conjunction with the depth of the boundary between the surface and this
588 subsurface feature, and in high latitudes, DL, and DVM may be the key to the establishment and
589 persistence of biological hotspots worldwide, by increasing the residence times of zooplankton
590 populations that serve as persistent food sources for higher trophic levels.

591 **Acknowledgments, Samples, and Data**

592 This project was funded through the National Science Foundation, Award Number
593 1744884 to UD and 1745011 to ODU. Computer simulations were run on the Wahab High
594 Performance computing cluster at ODU. We are grateful to the Antarctic Support Contractor and
595 their teams in Denver, CO, aboard the RVIB Laurence M. Gould, and at Palmer Station, without
596 whom a project such as this would not be possible. We thank the students and field assistants
597 from both projects for their valuable work on this project and the Palmer Antarctica Long-Term
598 Ecological Research team for their involvement, suggestions, and collaboration. We also thank
599 the NOAA Antarctic Marine Living Resources (AMLR) team at NOAA SWFSC and Dr.
600 Damien Guihen for their collaboration and assistance calibrating the Imaginex853 sensors. A
601 special thank you to Dr. Christian Riess (AMLR) for supplying the Nortek Signature 100 used in
602 this analysis.

603 ROMS particle simulations, mooring data, and Imaginex853 data matched to glider data
604 will be archived at BCO-DMO (http://www.bco-dmo.org/) after the manuscript is accepted.

References

Ainley, D. G. (2002). *The Adelie Penguin, Bellwether of Climate Change.* New York: Columbia University Press.

Batchelder, H. P., Edwards, C. A., & Powell, T. M. (2002). Individual-based models of copepod populations in coastal upwelling regions: implications of physiologically and environmentally influenced diel vertical migration on demographic success and nearshore retention. *Progress in Oceanography*, *53*(2), 307–333. https://doi.org/10.1016/S0079-6611(02)00035-6

Benoit, D., Simard, Y., Gagné, J., Geoffroy, M., & Fortier, L. (2010). From polar night to midnight sun: photoperiod, seal predation, and the diel vertical migrations of polar cod (Boreogadus saida) under landfast ice in the Arctic Ocean. *Polar Biology*, *33*(11), 1505–1520. https://doi.org/10.1007/s00300-010-0840-x

Bernard, K. S., & Steinberg, D. K. (2013). Krill biomass and aggregation structure in relation to tidal cycle in a penguin foraging region off the Western Antarctic Peninsula. *ICES Journal of Marine Science*, *70*(4), 834–849. https://doi.org/10.1093/icesjms/fst088

Bernard, Kim S., Cimino, M., Fraser, W., Kohut, J., Oliver, M. J., Patterson-Fraser, D., et al. (2017). Factors that affect the nearshore aggregations of Antarctic krill in a biological hotspot. *Deep Sea Research Part I: Oceanographic Research Papers*, *126*, 139–147. https://doi.org/10.1016/j.dsr.2017.05.008

Brierley, A. S. (2004). Diel vertical migration. *Current Biology*, *24*(22), 3.

Brinton, E., & Antezana, T. (1984). STRUCTURES OF SWARMING AND DISPERSED POPULATIONS OF KRILL (EUPHAUSIA SUPERBA) IN SCOTIA SEA AND SOUTH SHETLAND WATERS DURING JANUARY–MARCH 1981, DETERMINED BY BONGO NETS. *Journal of Crustacean Biology*, *4*, 45–66.

Carr, S. (2003). *The influence of Diel Vertical Migration on the Retention of Krill and Other Zooplankton in the Monterey Bay Region* (Thesis). Monterey Bay Aquarium Research Institute.

Carr, S. (2006). *The influence of vertical migratory behaviors on the transport of marine organisms* (PhD Dissertation). University of North Carolina Chapel Hill, Chapel Hill.

Carvalho, F., Kohut, J., Oliver, M. J., Sherrell, R. M., & Schofield, O. (2016). Mixing and phytoplankton dynamics in a submarine canyon in the West Antarctic Peninsula: PHYTOPLANKTON DYNAMICS IN WAP CANYON. *Journal of Geophysical Research: Oceans*, *121*(7), 5069–5083. https://doi.org/10.1002/2016JC011650

633 Carvalho, F., Kohut, J., Oliver, M. J., & Schofield, O. (2017). Defining the ecologically relevant mixed-layer depth
634 for Antarctica's coastal seas: MLD in Coastal Antarctica. *Geophysical Research Letters*, *44*(1), 338–345.
635 https://doi.org/10.1002/2016GL071205
636 Carvalho, F., Fitzsimmons, J. N., Couto, N., Waite, N., Gorbunov, M., Kohut, J., et al. (2020). Testing the Canyon
637 Hypothesis: Evaluating light and nutrient controls of phytoplankton growth in penguin foraging hotspots
638 along the West Antarctic Peninsula. *Limnology and Oceanography*, *65*(3), 455–470.
639 https://doi.org/10.1002/lno.11313
640 Cisewski, B., Strass, V. H., Rhein, M., & Krägefsky, S. (2010). Seasonal variation of diel vertical migration of
641 zooplankton from ADCP backscatter time series data in the Lazarev Sea, Antarctica. *Deep Sea Research*
642 *Part I: Oceanographic Research Papers*, *57*(1), 78–94. https://doi.org/10.1016/j.dsr.2009.10.005
643 Cleary, A., Durbin, E., Casas, M., & Zhou, M. (2016). Winter distribution and size structure of Antarctic krill
644 Euphausia superba populations in-shore along the West Antarctic Peninsula. *Marine Ecology Progress*
645 *Series*, *552*, 115–129. https://doi.org/10.3354/meps11772
646 Cohen, J. H., & Forward, R. B. (2005). Diel vertical migration of the marine copepod Calanopia americana. II.
647 Proximate role of exogenous light cues and endogenous rhythms. *Marine Biology*, *147*(2), 399–410. https://
648 doi.org/10.1007/s00227-005-1570-4
649 Conroy, J. A., Steinberg, D. K., Thibodeau, P. S., & Schofield, O. (2020). Zooplankton diel vertical migration
650 during Antarctic summer. *Deep Sea Research Part I: Oceanographic Research Papers*, *162*, 103324.
651 https://doi.org/10.1016/j.dsr.2020.103324
652 Couto, N., Kohut, J., Schofield, O., Dinniman, M., & Graham, J. (2017). Pathways and retention times in a
653 biologically productive canyon system on the West Antarctic Peninsula. *OCEANS 2017 - Anchorage*, 1–8.
654 Cresswell, K. A., Tarling, G. A., Thorpe, S. E., Burrows, M. T., Wiedenmann, J., & Mangel, M. (2009). Diel
655 vertical migration of Antarctic krill (Euphausia superba) is flexible during advection across the Scotia Sea,
656 *31*(10), 17.
657 Demer, D. A., & Hewitt, R. P. (1995). Bias in acoustic biomass estimates of Euphausia superba due to diel vertical
658 migration. *Deep Sea Research Part I: Oceanographic Research Papers*, *42*(4), 455–475.
659 https://doi.org/10.1016/0967-0637(94)E0005-C

660 Dinniman, M. S., Klinck, J. M., & Smith, W. O. (2011). A model study of Circumpolar Deep Water on the West
661 Antarctic Peninsula and Ross Sea continental shelves. *Deep Sea Research Part II: Topical Studies in*
662 *Oceanography*, *58*(13–16), 1508–1523. https://doi.org/10.1016/j.dsr2.2010.11.013
663 Emsley, S. M., Tarling, G. A., & Burrows, M. T. (2005). The effect of vertical migration strategy on retention and
664 dispersion in the Irish Sea during spring–summer. *Fisheries Oceanography*, *14*(3), 161–174.
665 https://doi.org/10.1111/j.1365-2419.2005.00327.x
666 Espinasse, B., Zhou, M., Zhu, Y., Hazen, E., Friedlaender, A., Nowacek, D., et al. (2012). Austral fall−winter
667 transition of mesozooplankton assemblages and krill aggregations in an embayment west of the Antarctic
668 Peninsula. *Marine Ecology Progress Series*, *452*, 63–80. https://doi.org/10.3354/meps09626
669 Everson I. (1983). Variations in vertical distribution and density of krill swarms in the vicinity of South Georgia, *27*,
670 84–92.
671 Fox, J., & Weisberg, S. (2019). *An {R} Companion to Applied Regression, Third Edition.* R, Thousand Oaks CA:
672 Sage. Retrieved from https://socialsciences.mcmaster.ca/jfox/Books/Companion/
673 Fraser, W. R., & Trivelpiece, W. Z. (1996). Factors controlling the distribution of seabirds: Winter-summer
674 heterogeneity in the distribution of adélie penguin populations. In E. E. Hofmann, R. M. Ross, & L. B.
675 Quetin (Eds.), *Antarctic Research Series* (Vol. 70, pp. 257–272). Washington, D. C.: American
676 Geophysical Union. https://doi.org/10.1029/AR070p0257
677 Goodrich, C. (2018). *SUSTAINED GLIDER OBSERVATIONS OF ACOUSTIC SCATTERING SUGGEST*
678 *ZOOPLANKTON PATCHES ARE DRIVEN BY VERTICAL MIGRATION AND SURFACE ADVECTIVE*
679 *FEATURES IN PALMER CANYON, ANTARCTICA* (Thesis). University of Delaware.
680 Graham, J. A., Dinniman, M. S., & Klinck, J. M. (2016). Impact of model resolution for on-shelf heat transport
681 along the West Antarctic Peninsula. *Journal of Geophysical Research: Oceans*, *121*(10), 7880–7897.
682 https://doi.org/10.1002/2016JC011875
683 Guihen, D., Fielding, S., Murphy, E. J., Heywood, K. J., & Griffiths, G. (2014). An assessment of the use of ocean
684 gliders to undertake acoustic measurements of zooplankton: the distribution and density of Antarctic krill
685 (Euphausia superba) in the Weddell Sea. *Limnology and Oceanography: Methods*, *12*(6), 373–389. https://
686 doi.org/10.4319/lom.2014.12.373

687 Haidvogel, D. B., Arango, H., Budgell, W. P., Cornuelle, B. D., Curchitser, E., Di Lorenzo, E., et al. (2008). Ocean
688 forecasting in terrain-following coordinates: Formulation and skill assessment of the Regional Ocean
689 Modeling System. *Journal of Computational Physics*, *227*(7), 3595–3624.
690 https://doi.org/10.1016/j.jcp.2007.06.016
691 Hays, G. C. (1995). Ontogenetic and seasonal variation in the diel vertical migration of the copepods Metridia
692 lucens and Metridia longa. *Limnology and Oceanography*, *40*(8), 1461–1465.
693 https://doi.org/10.4319/lo.1995.40.8.1461
694 Hays, G. C. (2008). A review of the adaptive significance and ecosystem consequences of zooplankton diel vertical
695 migrations. *Hydrobiologica*, *503*, 163–170.
696 Hazen, E., Suryan, R., Santora, J., Bograd, S., Watanuki, Y., & Wilson, R. (2013). Scales and mechanisms of marine
697 hotspot formation. *Marine Ecology Progress Series*, *487*, 177–183. https://doi.org/10.3354/meps10477
698 Hobbs, L., Cottier, F., Last, K., & Berge, J. (2018). Pan-Arctic diel vertical migration during the polar night. *Marine*
699 *Ecology Progress Series*, *605*, 61–72. https://doi.org/10.3354/meps12753
700 Hobbs, L., Banas, N. S., Cohen, J. H., Cottier, F. R., Berge, J., & Varpe, Ø. (2021). A marine zooplankton
701 community vertically structured by light across diel to interannual timescales. *Biology Letters*, *17*(2),
702 20200810. https://doi.org/10.1098/rsbl.2020.0810
703 Holland, D. M., & Jenkins, A. (1999). Modeling Thermodynamic Ice–Ocean Interactions at the Base of an Ice Shelf.
704 *JOURNAL OF PHYSICAL OCEANOGRAPHY*, *29*, 15.
705 Hudson, K. (2021). Krill Swarm ID RShiny Initial Release (Version v1.0.0). Zenodo.
706 https://doi.org/10.5281/ZENODO.4694333
707 Hudson, K., Oliver, M. J., Bernard, K., Cimino, M. A., Fraser, W., Kohut, J., et al. (2019). Reevaluating the Canyon
708 Hypothesis in a Biological Hotspot in the Western Antarctic Peninsula. *Journal of Geophysical Research:*
709 *Oceans*, *124*(8), 6345–6359. https://doi.org/10.1029/2019JC015195
710 Hudson, K., Oliver, M. J., Kohut, J., Dinniman, M. S., Klinck, J., Moffat, C., et al. (2021). A Recirculating Eddy
711 Promotes Subsurface Particle Retention in an Antarctic Biological Hotspot, *Preprint*.
712 https://doi.org/10.1002/essoar.10506313.1
713 Johnston, T. M. S., & Rudnick, D. L. (2009). Observations of the Transition Layer. *Journal of Physical*
714 *Oceanography*, *39*(3), 780–797. https://doi.org/10.1175/2008JPO3824.1

715 Kane, M. K., Yopak, R., Roman, C., & Menden-Deuer, S. (2018). Krill motion in the Southern Ocean: quantifying
716 in situ krill movement behaviors and distributions during the late austral autumn and spring: Krill motion in
717 the Southern Ocean. *Limnology and Oceanography*, *63*(6), 2839–2857. https://doi.org/10.1002/lno.11024
718 Kavanaugh, M., Abdala, F., Ducklow, H., Glover, D., Fraser, W., Martinson, D., et al. (2015). Effect of continental
719 shelf canyons on phytoplankton biomass and community composition along the western Antarctic
720 Peninsula. *Marine Ecology Progress Series*, *524*, 11–26. https://doi.org/10.3354/meps11189
721 Kelley, D., & Richards, C. (2020). oce: Analysis of Oceanographic Data (Version R package version 1.2-0).
722 Retrieved from https://CRAN.R-project.org/package=oce
723 Kils, U. (1981). Swimming behaviour, swimming performance and energy balance of Antarctic krill Euphausia
724 superba. *Biomass Science Series*, *3*, 1–121.
725 Kohut, J. T., Winsor, P., Statscewich, H., Oliver, M. J., Fredj, E., Couto, N., et al. (2018). Variability in summer
726 surface residence time within a West Antarctic Peninsula biological hotspot. *Philosophical Transactions of*
727 *the Royal Society A: Mathematical, Physical and Engineering Sciences*,
728 *376*(2122), 20170165. https://doi.org/10.1098/rsta.2017.0165
729 Lavoie, D., Simard, Y., & Saucier, F. J. (2000). Aggregation and dispersion of krill at channel heads and shelf
730 edges: the dynamics in the Saguenay - St. Lawrence Marine Park. *Canadian Journal of Fisheries and*
731 *Aquatic Sciences*, *57*(9), 1853–1869. https://doi.org/10.1139/f00-138
732 Marta-Almeida, M., Dubert, J., Peliz, Á., & Queiroga, H. (2006). Influence of vertical migration pattern on retention
733 of crab larvae in a seasonal upwelling system. *Marine Ecology Progress Series*, *307*, 1–19.
734 https://doi.org/10.3354/meps307001
735 McGeady, R., Lordan, C., & Power, A. (2019). Twilight migrators: factors determining larval vertical distribution in
736 Nephrops norvegicus with implications for larval retention. *Marine Ecology Progress Series*, *631*, 141–
737 155. https://doi.org/10.3354/meps13142
738 Nowacek, D. P., Friedlaender, A. S., Halpin, P. N., Hazen, E. L., Johnston, D. W., Read, A. J., et al. (2011). Super-
739 Aggregations of Krill and Humpback Whales in Wilhelmina Bay, Antarctic Peninsula. *PLoS ONE*, *6*(4),
740 e19173. https://doi.org/10.1371/journal.pone.0019173
741 Padman, L., Fricker, H. A., Coleman, R., Howard, S., & Erofeeva, L. (2002). A new tide model for the Antarctic ice
742 shelves and seas. *Annals of Glaciology*, *34*, 247–254. https://doi.org/10.3189/172756402781817752

743 Peterson, W. (1998). Life cycle strategies of copepods in coastal upwelling zones. *Journal of Marine Systems*, *15*(1),
744 313–326. https://doi.org/10.1016/S0924-7963(97)00082-1
745 Piñones, A., Hofmann, E., Daly, K., Dinniman, M., & Klinck, J. (2013). Modeling the remote and local connectivity
746 of Antarctic krill populations along the western Antarctic Peninsula. *Marine Ecology Progress Series*, *481*,
747 69–92. https://doi.org/10.3354/meps10256
748 Powers, J. G., Manning, K. W., Bromwich, D. H., Cassano, J. J., & Cayette, A. M. (2012). A DECADE OF
749 ANTARCTIC SCIENCE SUPPORT THROUGH AMPS. *Bulletin of the American Meteorological Society*,
750 *93*(11), 1699–1712.
751 R Core Team. (2020). *R: A language and environment for statistical computing*. Vienna, Austria: R Foundation for
752 Statistical Computing. Retrieved from www.R-project.org
753 Schofield, O., Ducklow, H., Bernard, K., Doney, S., Patterson-Fraser, D., Gorman, K., et al. (2013). Penguin
754 Biogeography Along the West Antarctic Peninsula: Testing the Canyon Hypothesis with Palmer LTER
755 Observations. *Oceanography*, *26*(3), 204–206. https://doi.org/10.5670/oceanog.2013.63
756 Sha, Y., Zhang, H., Lee, M., Björnerås, C., Škerlep, M., Gollnisch, R., et al. (2020). Diel vertical migration of
757 copepods and its environmental drivers in subtropical Bahamian blue holes. *Aquatic Ecology*.
758 https://doi.org/10.1007/s10452-020-09807-4
759 Smith, R. C., Baker, K. S., Fraser, W. R., Hofmann, E. E., Karl, D. M., Klinck, J. M., et al. (1995). The Palmer
760 LTER: A Long-Term Ecological Research Program at Palmer Station, Antarctica. *Oceanography*, *8*(3), 77–
761 86.
762 Tarling, G., Jarvis, T., Emsley, S., & Matthews, J. (2002). Midnight sinking behaviour in Calanus finmarchicus: a
763 response to satiation or krill predation? *Marine Ecology Progress Series*, *240*, 183–194.
764 https://doi.org/10.3354/meps240183
765 Tarling, G. A., & Johnson, M. L. (2006). Satiation gives krill that sinking feeling. *Current Biology*, *16*(3), R83–R84.
766 https://doi.org/10.1016/j.cub.2006.01.044
767 Tarling, G. A., & Thorpe, S. E. (2017). Oceanic swarms of Antarctic krill perform satiation sinking. *Proceedings of*
768 *the Royal Society B: Biological Sciences*, *284*(1869), 20172015. https://doi.org/10.1098/rspb.2017.2015

769 Tarling, G. A., Thorpe, S. E., Fielding, S., Klevjer, T., Ryabov, A., & Somerfield, P. J. (2018). Varying depth and
770 swarm dimensions of open-ocean Antarctic krill Euphausia superba Dana, 1850 (Euphausiacea) over diel
771 cycles. *Journal of Crustacean Biology*. https://doi.org/10.1093/jcbiol/ruy040
772 Thibodeau, P. S. (2015, October). *Diel Vertical Distribution Patterns of Zooplankton along the Western Antarctic*
773 *Peninsula*. Poster presented at the VIMS 75th Anniversary Alumni Research Symposium.

774